Hydrodynamic identification of NAUTILUS FOWT platform from small scale tests

V. Nava

Tecnalia Research and Innovation, Derio, Spain and Basque Centre for Applied Mathematics (BCAM), Bilbao, Spain

J. Galván, M. Sánchez-Lara, C. Garrido-Mendoza & G. Pérez-Morán

Tecnalia Research and Innovation, Derio, Spain

M. Le Boulluec & B. Augier

IFREMER, Marine Structures Laboratory, Plouzané, France

R. Rodriguez-Arias

Tecnalia Research and Innovation, Derio, Spain and NAUTILUS Floating Solutions, Derio, Spain

ABSTRACT: A small-scale tank test campaign of the NAUTILUS offshore wind floating semisubmersible platform was held at the Ifremer Deep Water Basin within the framework of the MaRINET 2 project. The support structure consists in four stabilized columns on a square pontoon supporting a generic 8-MW wind turbine. The tests were carried out at 1:36 Froude scale in parked conditions, and the mooring system was modelled as a set of aerial mooring springs providing a nonlinear stiffness.The hydrodynamic characterization of the floater from experimental data was tackled by using traditional techniques in naval architecture), as well as approaches derived from operational modal analysis in the frequency domain, such as the Sub Space Identification – Covariance (SSI-COV) method. The validity of this approach and its potential application to the identification of such kind of structures is discussed against the results of a more traditional technique based on the fitting of decay tests.

1 INTRODUCTION

Floating support structures for wind turbine often require the hydrodynamic characterization of the floater in order to calibrate and validate the numerical model for the simulation of the behavior of the platform. Canonical

methods, derived from the naval architecture sector and based on the fitting of the response to the analytical solution of a linear system subject to impulse excitation, have been applied in the last years to small scale model physical tests of such kind of platforms and devices in order to identify the main characteristics of the platform ((Nava, V. et al., 2014), (Uzunoglu et al., 2016)), i.e., by follow a linear approach for the detection of the natural periods and the linear damping, but in some cases also corrected with quadratic damping terms in order to take into account nonlinear phenomena. For example, in case of semisubmersible platforms for offshore wind support structures, see (Le Boulluec et al., 2013; Martin et al., 2014; Nielsen et al., 2006; Roddier et al., 2010; Skaare et al., 2007). Nava et al. (Nava, V. et al., 2014) applied classical procedures for identifying linear and nonlinear hydrodynamic properties of a first concept of the NAUTILUS platform ("Misión y Visión | NAUTILUS Floating Solutions," n.d.) from tank testing. In general, the traditional procedures are simple to implement and provide a good estimation of the parameters; however, in order to achieve a reliable assessment of the hydrodynamic characteristics of the floater, usually free and moored decay tests need to be performed reducing coupling among degrees of freedom, i.e. requiring a high level of precision, difficult to obtain sometimes due to the dimensions of the model, as well as it is convenient to carry them out under a wide set of initial conditions in order to achieve a good assessment of the hydrodynamic properties close to the resonance including some nonlinear effects. Moreover, the estimation of damping far from resonance frequency is not achieved by the classical fit of data. This results in the need of the technical community involved in the sector to detect procedures that can provide information about the hydrodynamic characteristics of the platform from indirect measurements, i.e. response of the platform under a more generic excitation, i.e. not needing controlled conditions which could be difficult to achieve in open sea (in case of full scale models) or due to the dimensions of the prototype in tanks. The Operational Modal Analysis (OMA) methods, by making use of only response under white noise or broadband excitation, have been often used in several engineering sectors for the structural identification of several kinds of structures: bridges, towers and buildings, as well other kinds of offshore structures. A review of the methods is presented in (Peeters and De Roeck, 2001). The methods can be classified into: Frequency-Domain Spectrum-Driven Methods, such as the Peak-Picking (PP) method, the Complex Mode Indication Function (CMIF) or the Frequency Domain decomposition (FDD) method and the Maximum Likelihood Identification (ML); and Time-Domain Covariance-Driven Methods, such as the Instrumental Variable

Method (IV), the Covariance-Driven Stochastic Subspace Identification (SSI-COV) method; and Time-Domain Data-Driven Methods, such as the Data-Driven Stochastic Subspace Identification (SSI-DATA).

Only few authors have applied these methods to offshore structures, see for example (Liu et al., 2015). In this paper the authors applied the SSI-DATA method to a real four-leg jacket-type offshore platform located in China.

Ruzzo et al. ((Ruzzo et al., 2017), (Ruzzo et al., 2016a)) have proposed a procedure, based on the Frequency Domain Decomposition (FDD) method for Operational Modal Analysis, which was verified numerically (Ruzzo et al., 2017) against numerical simulations in ANSYS AQWA v.16.0 on a simple spar-type structure and validated experimentally against intermediate scale data (Ruzzo et al., 2016a)on a 1:30 scale model of the OC3-Hywind prototype at the NOEL laboratory (Ruzzo et al., 2016b). The results obtained match well with numerical predictions and experimental data, and it seems that the FDD approach does provide sufficiently accurate results in case of broadband processes.

In this paper, the identification problem of an offshore wind floating semisubmersible support structure, developed by NAUTILUS Floating Solutions is tackled, by exploiting the data obtained during the experimental campaign held in January 2018 at the Ifremer Deep Water Basin within the framework of the MaRINET 2 project ("MaRINET2 Offshore Renewable Energy Testing | MaRINET Infrastructures Network," n.d., p. 2). The campaign included decay tests, regular and irregular wave tests, besides forced oscillations, for a wide range of initial conditions, wave height, wave periods and amplitudes and periods of the forced motions. The measured signals were the incoming waves (during regular and irregular wave tests), the displacements of the platform, the surface elevation at the columns and the pressure at the pontoon, as well as the forces at the legs of hexapod during the forced motions tests.

The SSI-COV method has been applied to white noise excitation in order to identify the heave and pitch characteristics and the results compared with those obtained by a time domain postprocess of decay tests. The validity of the approach and its potential application to the identification of such kind of structures is therefore discussed.

2 THE EXPERIMENTAL CAMPAIGN

The experimental campaign took place at the Deep Wave Basin – IFREMER in Brest, France. The basin is 50m long, 12.5m wide and 10m deep. The capacity for generating waves is for longitudinal regular and irregular waves heights up to 0.55 m. The facility is provided with a hexapod, so that the forced oscillation tests were carried out.

The choice of model scale is depending on several parameters, and it is typically governed by the following factors (see also Sect. 10.9 of (Det Norske Veritas (DNV), 2010)) such as:

- Limitations of model basin, e.g. tank size (area and water depth) and ceiling height, and its capability of generating the environmental conditions;
- The minimum load magnitude and load variation that the actuator(s) can accurately apply on the model.
- Possibility to properly model (at chosen scale, and with the required accuracy) hydrodynamic forces and phenomena that are important for the results with the available wave maker and current generation facilities.
- Whether scaling of results can be performed based on proven model laws and empirical corrections.
- Whether acceptable measuring accuracies can be obtained.

Large scales are often limited by the laboratory size, its capabilities to generate the environmental conditions, and practical/economic considerations. The size of the rotor can also be limited by the area spanned by the wind generator in the laboratory. Smaller scales are often limited by the increased uncertainties and less repeatability in the modelling, as well as larger scaling effects. Given all the above mentioned factors, the physical tests were carried out at 1:36 Froude scale in parked rotor conditions.

2.1 *The prototype and the experimental settings*

The design of the NAUTILUS support structure is based on four stabilized columns mounted on a square ring pontoon for a generic 8-MW wind turbine; the mooring system was modelled as a set of aerial mooring springs for the station keeping of the platform and providing a nonlinear stiffness to the support structure.

Because of the presence of the hexapod in some of the tests, it was not possible to include in those tests a tower/mast; this made impossible to achieve the objective moment of inertia in pitch and roll, and another configuration of the ballast in the platform was required. However, during the tests in which the use of the

hexapod was not required, a mast was included. This configuration was named “With Tower (WT)”, i.e. it is the configuration with tower installed. In this configuration. free and moored decay tests, regular and irregular wave tests were carried out.

A sketch of the model WT tested during the tests with waves (regular and irregular) is reported in Figure 1, as well as the set of the horizontal series of springs acting as restoring system. In Covariance-Driven Stochastic Subspace Identifica-tion (SSI-COV) method

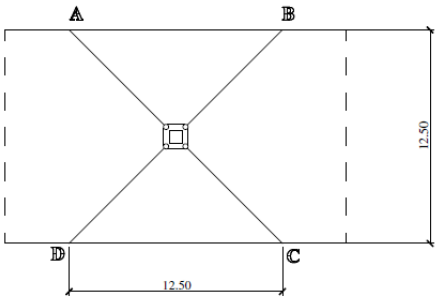

a

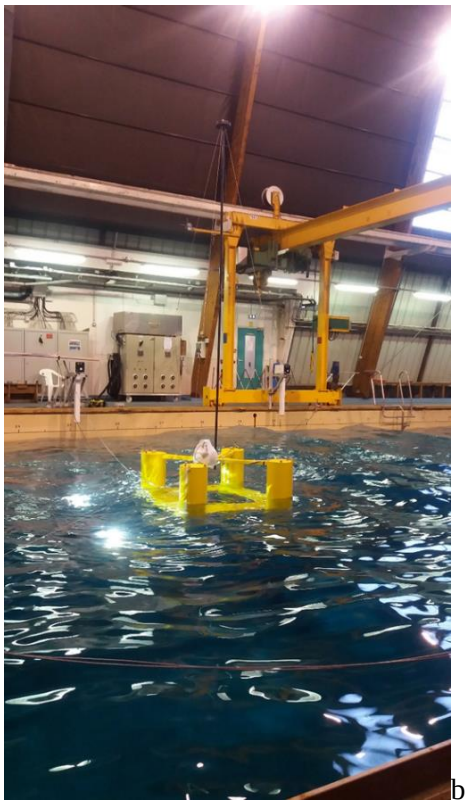

b

Figure 1: Configuration of the NAUTILUS platform WT (with tower) in the tank at Brest. a) plan view of the platform in the tank and moorigns; b) photo of the scaled model in the tank

A full review of the method can be found in (Peeters and De Roeck, 2001), whilst a comprehen-sive description of the algorithm related to some ap-plication can be found, for example in (Magalhães and Cunha, 2011) and (Nord et al., 2017).

Table 1: Key Geometrical parameters and displacement (scaled at 1:36 Froude length scale) of the WT model configuration.

		Full Scale	Scale 1:36
Floater dimensions and displacement	Column diameter [m]	11	0.306
	Distance between columns [m]	41	1.139
	Column height [m]	32	0.889
	Displacement [t]	11538	0.247

Table 1, the non-sensitive full-scale key geometrical parameters of the platform are reported, as well as the values of the 1:36 scaled prototype are reported. The displacement of the platform is also reported. The mooring system was aerial and consisted in four lines. Each line was made of a set of linear springs, in order to adjust the full system to the objective stiffness. The springs acted mostly in the horizontal direction and the stiffness of the aerial spring mooring system (in scale 1:36) is shown in Figure 2.

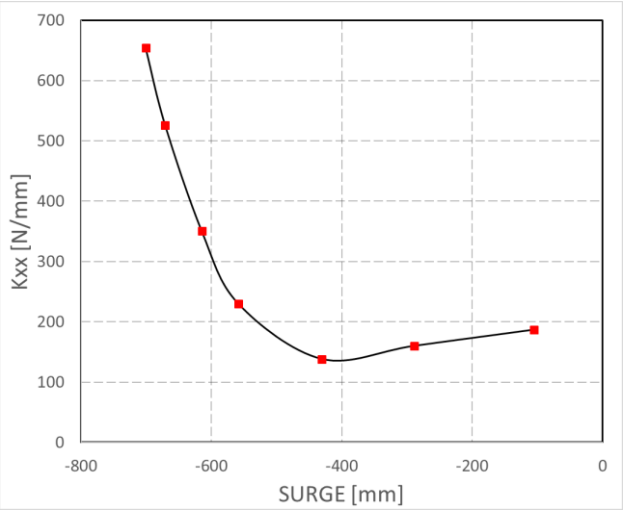

Figure 2: Measured surge/sway stiffness of the aerial mooring system (scale 1:36)

Several quantities were directly measured. When possible, redundant measurements will be required to reduce the uncertainties.

The following parameters have been monitored:

- Displacements in 6 degrees of freedom;
- Pressures (three pressure gauges were installed at the pontoon);
- Wave elevation at different points;
- Stroke of the hexapod for the tests in which it was active.

Use of treatment of data during the post-process of the outcome of the campaign can be adopted for the indirect measure of quantities and thus verifying advanced numerical models and the reliability in the measurements.

2.2 *The test campaign*

The duration of the campaign was 10 working days. During this campaign, the following tests were performed:

- Static or steady state characterization of the physical model of the platform;
- Free decay Tests – for different initial displacement, smaller and larger ones;
- Moored Decay Tests: however, the mooring system which will be considered is aerial, and the chain behavior modelled as springs. As for the free decay tests, they were carried out for different initial displacement, smaller and bigger ones.
- Forced Oscillation Tests, given the presence of a hexapod allowing the superimposition of motions to the platform, there were considered three periods and two amplitudes for three degrees of freedom (the symmetry of the model was taken into consideration).
- Tests in regular waves, for two amplitudes and five periods.
- Tests in spectrum compatible waves, both in operational and extreme conditions.

No wind excitation was considered. As for the spectrum compatible excitation, both white noise spectra and mean JONSWAP spectra were considered. Decay and forced oscillation tests were carried out under two configurations of the platform, i.e. considering some ancillary parts for damping enhancement.

3 THE IDENTIFICATION METHODS

Two identification methods have been proposed in this work to assess the hydrodynamic characteristics of the platform in heave and pitch.

The first method is based on the fit of data (decay tests), and it was already used in (Nava, V. et al., 2014) for the estimation of the linear characteristics on a previous prototype of the NAUTILUS platform during an experimental campaign held at the wave tank in Cork in January 2014.

The second method is based on the Subspace Identification Method, when the structure is applied to white noise excitation.

3.1 *Fit of impulse response*

The method is based on the analytical representation of the response of a rigid body to an impulse excitation. If excited by an impulse in a given direction, indeed, the response of a rigid body in such degree of freedom follows the following form:

$$y = y_o \, exp(-\alpha t) \, cos(t/\tau) \qquad (1)$$

Where y is the response (heave or pitch motion), y_o represents the initial displacement, α is a dimensional coefficient related to damping and τ a time constant related to the oscillation period of the system. If y_i and y_{i+1} are two following peaks in time at the instants respectively t_i and t_{i+1}, then one can estimate the averaged values for $\bar{\alpha}$ and $\bar{\tau}$.:

$$\bar{\tau} = \frac{1}{N}\sum_{i=1}^{N} t_i - t_{i-1} \qquad (2)$$

and

$$\bar{\alpha} = \frac{1}{N}\sum_{i=0}^{N-1} \frac{\ln(y_i/y_{i+1})}{t_{i+1}-t_i} \qquad (3)$$

The estimation of the natural frequency and the percentage of critical damping is straightforward:

$$\omega_n = \sqrt{\bar{\alpha}^2 + (2\pi/\bar{\tau})^2} \qquad (4)$$

and

$$\zeta = \sqrt{1 - 1/(\omega_n \bar{\tau})^2} = \frac{\bar{\alpha}}{\omega_n} \qquad (5)$$

Finally, given values for the hydrostatic stiffness and added mass, then one can easily get an estimate for the additional damping and natural period.

3.2 *Covariance-Driven Stochastic Subspace Identification (SSI-COV) method*

A full review of the method can be found in (Peeters and De Roeck, 2001), whilst a comprehensive description of the algorithm related to some application can be found, for example in (Magalhães and Cunha, 2011) and (Nord et al., 2017).

A block Toeplitz matrix of the autocovariances is built:

$$T_{1|i} = \begin{bmatrix} R_i & R_{i-1} & \dots & R_1 \\ R_{i+1} & R_i & \dots & R_2 \\ \dots & \dots & \dots & \dots \\ R_{2i-1} & \dots & \dots & R_i \end{bmatrix} \quad \text{with} \quad i = 1, \dots, \{\text{Citation}\} j_b \qquad (6)$$

where the autocovariances are defined as:

$$R_i = \langle y(t) y(t + i\Delta t) \rangle \qquad (7)$$

The size of $T_{1|i}$ is $n_0 j_b x n_0 j_b$, where n_0 is the number of output and j_b is the order of the method.

Such a matrix can be decomposed as:

$$T_{1|i} = O\Gamma = USV^T \qquad (8)$$

where O is the extended observability matrix and Γ is the reversed extended stochastic controllability matrix. The third term in the equality represent the Single Value Decomposition to the Toeplitz matrix; thus:

$$O = US^{\frac{1}{2}} \tag{9}$$

$$\Gamma = S^{1/2}V^T \tag{10}$$

The output influence matrix C can be calculated as the first $n_0$rows of O, whilst the state space matrix A can be calculated, for example, as:

$$A = O^{to\dagger}O^{bo} \tag{11}$$

where O^{to} contains the first $n_0(j_b - 1)$ lines of O and O^{bo} contains the last $n_0(j_b - 1)$ lines of O and $O^{to\dagger}$ represents the Moore–Penrose pseudo-inverse of the matrix O^{to} and could be calculated as it follows:

$$O^{to\dagger} = (O^{to^T}O^{to})^{-1}O^{to^T} \tag{12}$$

If μ_k are the eigenvalues of A, then

$$\lambda_k = \frac{\mu_k}{\Delta t} \tag{13}$$

$$\omega_{n,k} = \frac{Abs(\lambda_k)}{2\pi} \tag{14}$$

$$\zeta = -\frac{Re(\lambda_k)}{Abs(\lambda_k)} \tag{15}$$

where Δt is the sampling period of the signals.

4 RESULTS AND DISCUSSION

All the signals were sampled at 100 Hz. In this work, the only degrees of freedom that have been considered were heave and pitch, in order to reduce the computational effort needed for the SSI-COV method. The results are all of them referred to the moored condition.

First of all the decay test in moored conditions for pitch have been considered. The time series is plotted in Figure 3 and the results are summarised in Table 2.

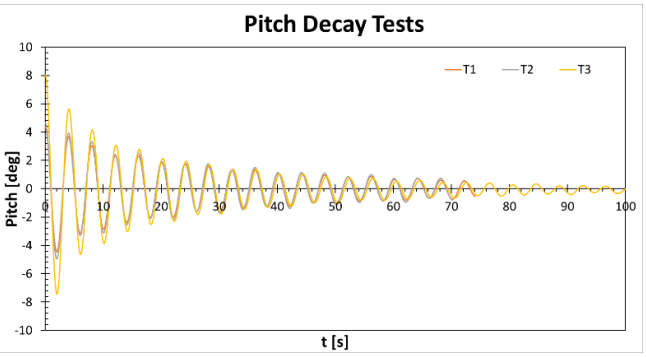

Figure 3:Time series of the pitch decay tests.

Table 2: Results of the pitch decay tests and statistics (all over the length of the signal)

	T1	T2	T3	Mean all signal	STD
Inital Point [mm]	4.38	4.66	8.03	-	-
To [s]	4.02	4.00	4.01	4.01	0.01
$\bar{\alpha}$	0.03	0.03	0.03	0.03	0.00
ω_n [rad/s]	1.56	1.57	1.57	1.57	0.00
Tn [s]	4.02	4.00	4.01	4.01	0.01
ζ	1.98%	1.68%	1.89%	1.85%	0%

The following considerations can be made:

- The tests were conducted under different initial conditions; nevertheless, the dispersion in terms of oscillation period and average linear damping coefficient is extremely small and this means that the test was well performed;
- The damping is highly nonlinear. Indeed, the average damping coefficient obtained essentially from peaks after the third one is much lower than the one obtained just considering the first peak of the first three peaks. Just as an example, consider the values of the parameters obtained in the test T3 by considering only the first peak, the average of the first three peaks and all the signal in table 3

Table 3: Results of the pitch decay test T3 and mean of the parameters (first peak, three first peaks, all signal)

	First Peak Values	Mean Three Peaks	Mean All Signal
To [s]	4.07	4.06	4.01
$\bar{\alpha}$	0.09	0.08	0.03
ω_n [rad/s]	1.55	1.55	1.57
Tn [s]	4.06	4.05	4.01
ζ	5.61%	5.09%	1.89%

The heave decay test was even more controlled, because of the methodology of execution and its accuracy. This makes the outcome of the three tests T1, T2 and T3 even with less dispersion than the pitch ones, as it can be seen in Figure 4 and through the results in table 4. In Table 5, referred to test T3, it could be easily noticed that the nonlinear effects, which affected the pitch decay tests, are in this case even more emphasized.

As for the comparison with the outcome of the SSI-COV method, the moored structure subject to random waves has been considered. A pink noise power spectral density PSD has been considered, in the range [1.5 – 2.5] rad/s, as reported in Figure 5.

The responses of the structure, recorded by the acquisition system, are reported in Figure 6. They are 415 long, for a total of 41500 samples.

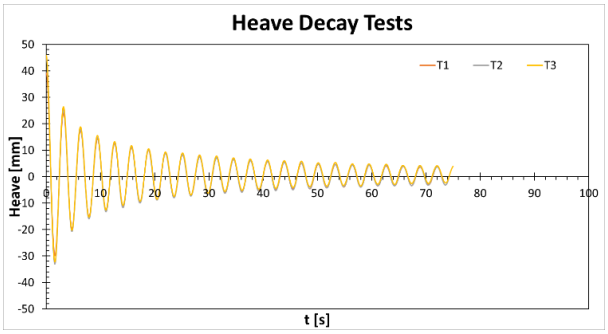

Figure 4:Time series of the heave decay tests.

Table 4: Results of the heave decay tests and statistics

	T1	T2	T3	MEAN	STD
Inital Point [mm]	39.14	45.24	45.93	-	-
To [s]	3.14	3.13	3.13	3.13	0.00

$\bar{\alpha}$	0.04	0.04	0.04	0.04	0.00
ω_n [rad/s]	2.00	2.01	2.01	2.01	0.00
Tn [s]	3.14	3.13	3.13	3.13	0.00
ζ	1.78%	1.83%	1.79%	1.80%	0.00

Table 5: Results of the heave decay test T3 and mean of the parameters (first peak, three first peaks, all signal)

	First Peak Values	Mean Three Peaks	Mean All Signal
To [s]	3.18	3.15	3.13
$\bar{\alpha}$	0.17	0.11	0.04
ω_n [rad/s]	1.98	2.00	2.01
Tn [s]	3.17	3.14	3.13
ζ	8.76%	5.71%	1.79%

The procedure described in Section 0 has been applied, but no optimal tuning of the algorithm has been carried out.

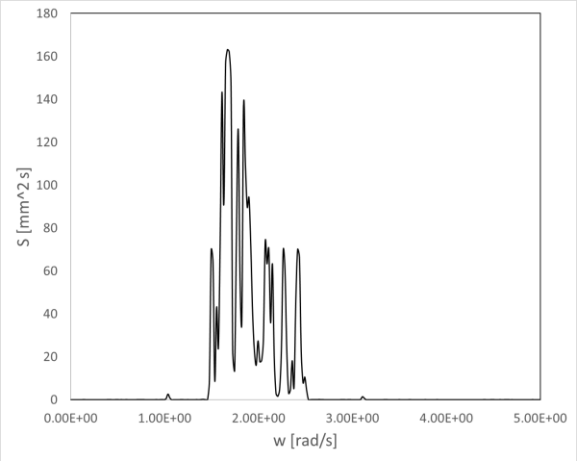

Figure 5: Power spectral density of the free surface displacement at test 31 (pink noise).

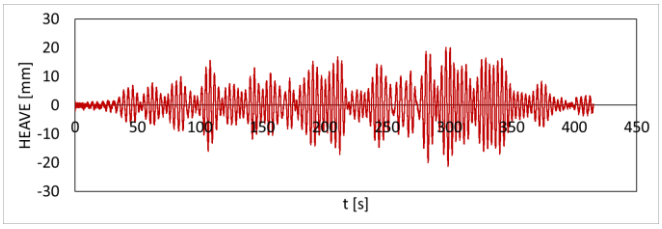

a

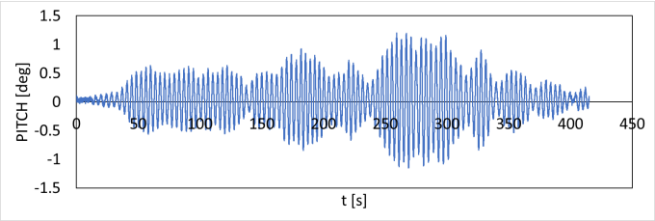

b

Figure 6:Time series of the heave (a) and pitch (b) displacements of the platform.

The maximum order of the model considered was 50. At each order, it would correspond a maximum of poles equal to the order. However, poles are complex conjugate and several poles are not “stable”, i.e. they are fictitious and they disappear while considering higher orders. Thus, the concept of stable poles should be introduced. According to our definition, one pole at a certain order is defined as stable if:

a) A close pole is present also for the 10 following orders;
b) two poles are considered to be close if they differ less than 1% in terms of frequency;
c) two poles are considered to be close if they differ less than 5% in terms of damping ratio.

The outcome of the procedure is shown in Figure 7, representing the stability diagram in terms of frequency. It can be easily seen that by following the strict criteria, two columns of stable modes have been identified: they occur at frequency close to the heave and pitch natural frequency, respectively. By averaging the frequencies of those poles, the results in Table 6 show that the natural period in pitch differs from the one detected from the previous procedure by only 0.5%, and in heave procedure by less than 2%. Worst results are obtained in terms of damping ratio, as it appears extremely low. Results in this sense are not shown and currently are still under investigation.

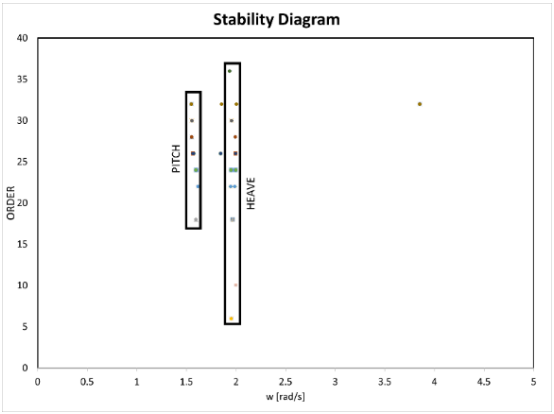

Figure 7: Stability diagram of the SSI-COV procedure as a function of the order of the method.

From the diagram in Figure 7, one can notice also the presence of stable spurious modes.

Table 6: Results of the natural period estimated from the response under white noise excitation through a SSI-COV procedure and estimation of the error.

Degree of freedom	Tn (SSI-COV) [s]	% ERR
Heave	3.19	1.9%
Pitch	3.99	0.5%

As aforesaid, the procedure and its parameters have not been optimally tuned, and this could be one of the reasons why not many poles have been identified. However, the consistency of the results with more traditional post process based on fitting of decay tests confirm the adequateness of the approach for detecting the natural frequency of this kind of support structures.

5 CONCLUSIONS AND FUTURE WORK

In this paper, the results of a small scale physical experimental campaign carried out at the Ifremer Deep Water basin on the NAUTILUS concept have been postprocessed by using: 1) a traditional technique, based on the fit of data of decay tests; 2) the SSI-COV approach, i.e. an approach derived from the field of the Operational Modal analysis, under the occurrence of pink-noised random waves. In both cases, only two degrees of freedom (namely, pitch and heave) have been considered for only demonstration purposes.

The main results of the work can be summarized as it follows:

- The quality of the data recorded during decay tests was pretty good;

- Decay tests, moreover, showed a great nonlinear behaviour for higher displacements.

- The SSI-COV procedure, even if not optimally tuned, was able to well predict the natural frequencies of the system, but it failed in terms of damping ratio. The reasons why this occurred are still under investigation.

It seems that the SSI-COV is a good approach to be used in real seas to identify the modes of the structures, and eventually detect changes in the properties of the floater (for example, increased mass due to fouling, etc.). However, in order to have a wider perspective of the range of the validity for the procedure, other studies are required, such as for example investigating the full system (6 degrees of freedom), the effects of the narrowness of the power spectrum, the length of the signals and the identification of the optimal tuning of the parameters of the model.

ACKNOWLEDGEMENTS

The authors gratefully acknowledge the financial support received from MARINET2, a European Community - Research Infrastructure Action funded by the European Union Horizon2020 programme under Grant Agreement 731084 and the support of the Basque Business Development Agency which made this work possible funding FLOW project – grant ZE-2017/00031.

First author's work is also supported by the Basque Government through the BERC 2018-2021 program and by Spanish Ministry of Economy and Competitiveness MINECO: BCAM Severo Ochoa excellence accreditation SEV-2013-0323.

REFERENCES

Det Norske Veritas (DNV), 2010. Environmental COnditions and Environmental Loads (No. DNV-RP-C205).

Le Boulluec, M., Ohana, J., Martin, A.& Houmard, A., 2013. Tank Testing of a New Concept of Floating Offshore Wind Turbine, *ASME 2013 32nd International Conference on Ocean, Offshore and Arctic Engineering*. American Society of Mechanical Engineers, pp. V008T09A100–V008T09A100.

Liu, F., Li, H., Hu & S.-L.J., 2015. Stochastic modal analysis for a real offshore platform, in: *Proceedings of the 6th International Operational Modal Analysis Conference*, Gijón, Spain. pp. 12–14.

Magalhães, F.& Cunha, Á., 2011. Explaining operational modal analysis with data from an arch bridge. *Mech. Syst. Signal* Process. 25, 1431–1450.

MaRINET2 Offshore Renewable Energy Testing | MaRINET Infrastructures Network [WWW Document], n.d. . MaRINET2. URL http://www.marinet2.eu/ (accessed 6.6.18).

Martin, H.R., Kimball, R.W., Viselli, A.M.& Goupee, A.J., 2014. Methodology for wind/wave basin testing of floating offshore wind turbines. *J. Offshore Mech. Arct. Eng.* 136, 020905.

Misión y Visión | NAUTILUS Floating Solutions, n.d.

Nava, V., Aguirre, G., Galvan, J., Sanchez-Lara, M., Mendikoa, I.& Perez-Moran, G., 2014. Experimental studies on the hydrodynamic behavior of a semi-submersible offshore wind platform, *Renewable Energies Offshore.* C. Guedes Soares (Ed.), Taylor & Francis Group, London, UK, pp. 709-715.

Nielsen, F.G., Hanson, T.D.& Skaare, B., 2006. Integrated dynamic analysis of floating offshore wind turbines, *25th International Conference on Offshore Mechanics and Arctic Engineering*. American Society of Mechanical Engineers, pp. 671–679.

Nord, T.S., Kvåle, K.A., Petersen, Ø.W., Bjerkås, M.& Lourens, E.-M., 2017. Operational modal analysis on a lighthouse structure subjected to ice actions. *Procedia Eng*. 199, 1014–1019.

Peeters, B.& De Roeck, G., 2001. Stochastic System Identification for Operational Modal Analysis: A Review. *J. Dyn. Syst. Meas. Control* 123, 659.

Roddier, D., Cermelli, C., Aubault, A.& Weinstein, A., 2010. WindFloat: A floating foundation for offshore wind turbines. *J. Renew. Sustain. Energy* 2, 033104.

Ruzzo, C., Failla, G., Collu, M., Nava, V., Fiamma, V.& Arena, F., 2017. Output-only identification of rigid body motions of floating structures: a case study. *Procedia Eng*. 199, 930–935.

Ruzzo, C., Failla, G., Collu, M., Nava, V., Fiamma, V.& Arena, F., 2016a. Operational Modal Analysis of a Spar-Type Floating Platform Using Frequency Domain Decomposition Method. *Energies* 9, 870.

Ruzzo, C., Fiamma, V., Nava, V., Collu, M., Failla, G.& Arena, F., 2016b. Progress on the experimental set-up for the testing of a floating offshore wind turbine scaled model in a field site. *Wind Eng.* 0309524X16660023.

Skaare, B., Hanson, T.D., Nielsen, F.G., Yttervik, R., Hansen, A.M., Thomsen, K.& Larsen, T.J., 2007. Integrated dynamic analysis of floating offshore wind turbines, in: 2007 *European Wind Energy Conference and Exhibition*.

Uzunoglu, E., Karmakar, D.& Guedes Soares, C., 2016. Floating Offshore Wind Platforms, in: Castro-Santos, L., Diaz-Casas, V. (Eds.), *Floating Offshore Wind Farms*. Springer International Publishing, Cham, pp. 53–76.